International Journal of Integrated Academic Research
ISSN : APPLIED | Volume-1 Issue-1 | Inaugural Edition | January-March 2026 | IAR11-006
doi:

CONTROL STRATEGY FOR GRID-CONNECTED PV SYSTEM UNDER MISMATCHED CONDITIONS

Dr. Sangeetha , *Associate Professor, Department of EEE,*
Priyadarshini Engineering College For Women, Khammam.

ABSTRACT: A transformerless single-phase PV inverter that is connected to the grid is the subject of this article. Regardless of the weather, it is capable of operating in either buck or boost mode and extracting the maximum amount of power from two subarrays that are connected in series. The inverter's dual buck and boost modes facilitate subarray assembly by connecting solar PV modules in series. Under specific weather conditions, the power output of the subarray is enhanced. The inverter's design and control system wholly eliminate high-frequency common mode voltage components. Due to this, solar panels continue to discharge current. It also performs well in all of its operations. Through an exhaustive examination of the system, a mathematical model results. The notion's feasibility is demonstrated through a multitude of modeling studies. The concept's feasibility is illustrated by the development and evaluation of a 1.5 kW laboratory prototype. Inclement weather, transformerless, boost, and buck solar inverters, grid-tied single-phase, and series-connected modules, as well as maximum power point tracking.

Keywords: *PV modules, PV inverter, boost, sub array, PV arrays.*

1. INTRODUCTION

A photovoltaic (PV) system optimizes the efficacy of each PV module in an array, regardless of temperature fluctuations or sunlight. Misaligned photovoltaic modules generate significantly less electricity. A solar array with numerous successive modules exacerbates mismatched environmental conditions (MEC).

In order to increase the input DC link voltage of the inverter in a grid-tied transformer-less photovoltaic system, additional modules must be connected in series. The power output of grid-connected transformer-less (GCT) photovoltaic systems, particularly single-phase GCT (SPGCT) inverter-based systems that employ H-bridge and NPC inverters, is influenced by maximum power point tracking (MEC).

MEC concerns in solar systems are addressed in the literature through a variety of methodologies. A comprehensive analysis of a variety of methodologies is offered. The power extraction of Maximum Efficiency Charge (MEC) can be improved by properly connecting photovoltaic (PV) modules or by utilizing an updated MPPT algorithm to monitor the global maximum power point (MPP) of the PV array. Nevertheless, these techniques are not feasible for low-power SPGCT PV systems. SPGCT systems should refrain from altering the electrical connections of solar modules, as this results in the addition of additional components and the complication of the system.

Power electronic equalization (PEE) or a DC-to-DC converter have been employed

to regulate photovoltaic modules in solar arrays. The goal is to optimize the power generation of PV modules while simultaneously managing MEC. The complexity and cost of the installation of a power electronic equalization system are increased by the presence of numerous components.

A generation control circuit (GCC) is the sole instrument utilized for this purpose, as it regulates power fluctuations between solar modules at their maximum power points (MPPs). Shunt current correction for each module and series voltage modulation for each PV string in a PV array are implemented to optimize power generation during MEC. A DC-to-DC converter is integrated into each solar module. Nevertheless, these systems are inefficient due to their numerous components and conversion processes. The same issues that affect power electronic equalization systems also affect them. A string is constructed by connecting a predetermined number of modules one after the other, rather than evaluating each module under MPP. MPP functions on www.jespublication.com after the strings have been modified. However, the control system's complexity and the number of components have remained constant. By employing procedures that enable each subarray to operate at its own optimum power point, each PV module is divided into two subarrays, thereby simplifying control settings and reducing the number of components.

In general, these methods have been unsuccessful. The SPGCT PV inverter may produce an increased amount of power during MEC due to surge and kickback phases. The number of PV modules required in series with a PV array decreases following the intermediate boost step. The operational efficiency of the proposed systems is considerably enhanced by the incorporation of high-frequency switches into the inverter and/or DC-to-DC converter stages. As a consequence, passive components are substantially diminished. The indicated effectiveness increases by 1% to 2% in comparison to previous statistics.

In this article, PV modules are divided into two subarrays that are connected in series. The optimal method of power harvesting during MEC is then determined by modulating each subarray using a buck-boost inverter.

When an input PV array is divided into two subarrays, the number of series-connected modules in each subarray is reduced in comparison to other methods. The inverter's topological design and control system are intended to limit the leakage current from PV arrays. The voltage stress on active devices is approximately 50% lower than that of the solutions that have been presented. This simplifies the operation of high-frequency equipment and minimizes switching losses.

As the frequency of operation increases, passive components become smaller. The design that has been recommended is effective. Although the European project's optimum efficiency is 97.65%, the anticipated efficiency is 97.02%.

2.PHOTOVOLTAIC INVERTER

Figure 2.1 illustrates the block diagram of a solar power generation system that is connected to the infrastructure. In order to convert light energy into DC, a photovoltaic (PV) module employs numerous PV cells. These are

indispensable for the generation of photovoltaic power. The DC output of solar panels is converted to AC electricity by an inverter. 3. infrastructure: The local electrical infrastructure purchases electricity generated by inverters. In order to optimize the quantity of electricity produced by solar modules, the power conversion device must implement maximum power point tracking (MPPT). MPPT systems continuously monitor the voltage at which the most electricity is consumed.

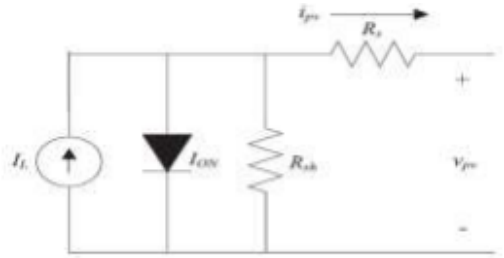

Fig1.Equivalent Circuit Diagram of PV Cell

$$i_{pv} = I_L - I_s[\exp[\alpha(v_{pv} + R_s i_{PV})] - 1] - \frac{v_{pv} + R_s i_{pv}}{R_{sh}}$$

MPPT:(MaximumPowerPointTracking)

Maximum power point tracking (MPPT) optimizes energy extraction in a diverse array of operational scenarios. MPPT enhances system efficiency and minimizes energy expenditures. MPPT algorithms must autonomously determine the maximum power point voltage or current of a solar array under specific temperature and irradiance conditions. There are numerous methods for performing MPPT. The majority of solutions react to both temperature and irradiance, while a small number of them react solely to temperature.

Pertur band Observe algorithm

The most frequently employed MPPT technique in photovoltaics is perturb and observe. The system sustained minor damage prior to this operation. The system will be similarly disrupted by an increase in output power. If the output power is reduced, the disturbance will be reversed. After meticulously modifying the array terminal voltage, the Perturb and Observe application compares the photovoltaic output power to the previous perturbation cycle. The PV array is reversed by the control system if the operational point remains constant, despite fluctuations in voltage and power. The method remains unchanged for the subsequent perturbation cycle. The operation of the algorithm is illustrated in Flow Chat 2.1. The perturb and observe method frequently encounters array terminal voltage variations during MPPT cycles. When the output power of the PV system reaches its maximum, power loss occurs. The PowerPoint presentation has been completed.

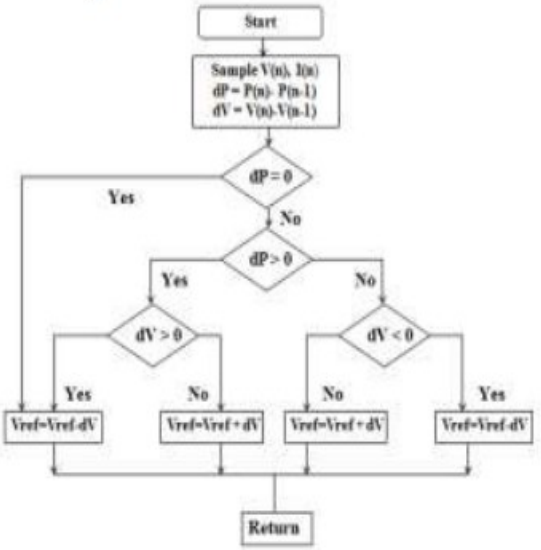

Flow Chart1:Perturb and Observe

3.DC-DCCONVERTERBASICS

A DC-to-DC converter is an electrical power device that has the capability of converting a DC input voltage to a DC output voltage. The voltage of DC sources is regulated by electromechanical devices or electric circuits. There have been reports of excessively low power levels

(resulting from miniature batteries) and excessively high power levels (resulting from high-voltage power transfer). The voltage level of the information is not consistent with the typical output. Furthermore, the utilization of DC-to-DC converters facilitates the regulation of force transmission and noise reduction. A compendium of typical topologies observed in DC-to-DC converters is provided below.

Boost Converter

Figure 3.6 schematically illustrates the fundamental boost converter. When the input voltage exceeds the intended output voltage, this circuit is implemented.

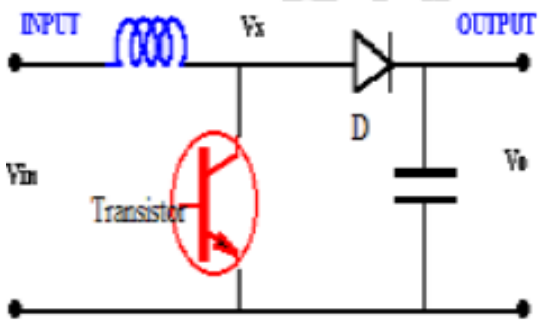

Fig Boost Converter Circuit

Vx is Vin when the transistor is ON and Vo when it is OFF, as indicated by the inductor current streaming through the diode. The term "continuous conduction" (CC) in this analysis denotes the assumption that the inductor current flows continuously. In order to maintain a constant average current, the average voltage across the inductor must be zero, as illustrated in Figure 3.7.

4. PROPOSED INVERTER AND ITS CONTROL

The Dual Buck & Boost Based Inverter (DBBI) circuit is comprised of the rectifying stage and dc-dc converter stage, as illustrated in Figure 2. The dc-to-dc converter stage's CONV1 and CONV2 supply electricity to the P V1 and P V2 subarrays of the solar photovoltaic array. Antiparallel body diodes D1 and D3, filter inductors and capacitors L1, Cf1, and Co1, as well as self-commutating switches S1 and D1, S3 and D3, free-wheeling diodes Df1 and Df3, and capacitors S1 and D3, are all included in the CONV1 sequence. An anti-parallel body diode D2 is situated above the CONV2 section, which also includes filter inductors and capacitors L2, Cf2, and Co2, as well as self-commutating switches S2. Body diodes and self-commutated switches (S5, S6, S7, and S8) comprise the inverting stage. The grid is connected to the inverter stage via the filter inductor, or Lg. The parasitic capacitance that travels from the solar array to the ground is replicated by the Cpv1 and Cpv2 capacitors.

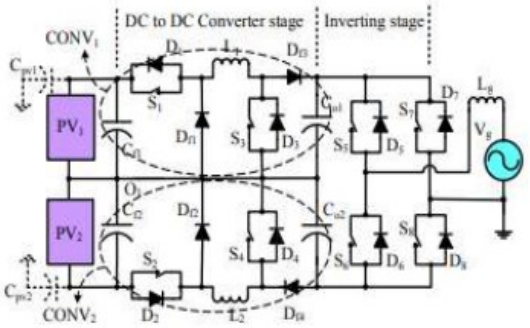

Dual Buck & Boost based Inverter (DBBI)

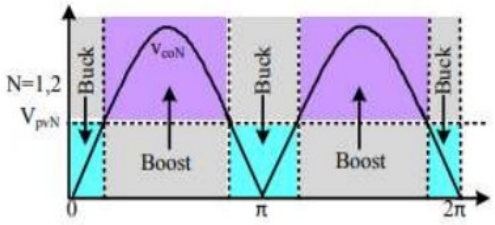

Buck stage and Boost stage of the proposed inverter

Figure 2 illustrates that CONV2 operates in buck mode when Vpv2 exceeds vco2. However, CONV1 operates in buck mode when Vpv1 is greater than or equal to vco1. The output voltages of CONV1 and CONV2 are Vco1 and Vco2, respectively,

in contrast to the MPP voltages of PV1 and PV2, which are denoted as Vpv1 and Vpv2, respectively. The constant state of switches S1 and S2 guarantees a sinusoidal grid current (ig) during the buck mode duty cycles. Assuming that Vpv1 is less than vco1, CONV1 enters boost mode; conversely, CONV2 enters boost mode when Vpv2 exceeds vco2. S3 and S4 are modulated sinusoidally to ensure sinusoidal IG while S1 and S2 are functioning in boost mode. In order to accomplish unity power factor operation, the sinusoidal switching signals of the CONV1 and CONV2 switches are synchronized with the grid voltage, vg. During the positive half cycle (PHC), switches S5 and S8 remain illuminated; conversely, switches S6 and S7 are perpetually disabled. Switches S6 and S7 remain illuminated during the negative half cycle (NHC), while switches S5 and S8 remain inactive. The figure illustrates the operation of the proposed inverter. 2.1. The MPP parameters undergo modifications when the insolation level and ambient temperature of subarray P V1 differ from those of subarray P V2.

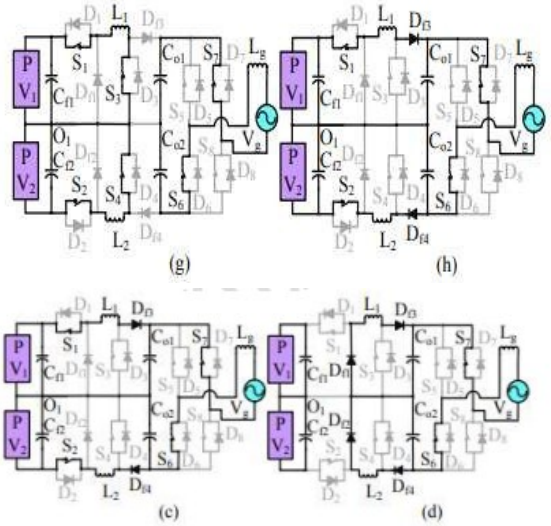

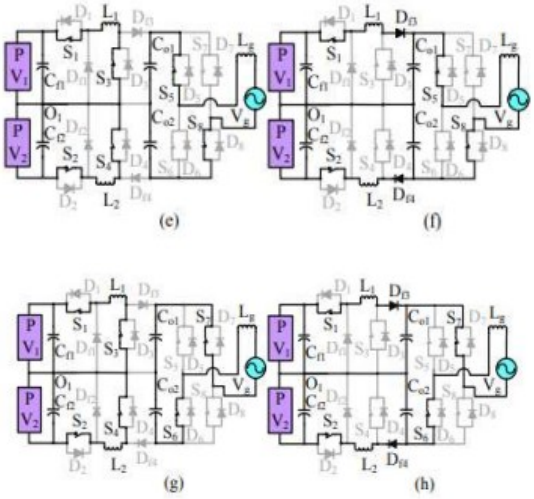

(a) PHC buck mode, (b) PHC buck mode, (c) PHC boost mode, (e) PHC boost mode, and (g) NHC boost mode are all examples of active and free-wheeling modes that the DBBI can be observed in during its operational phases. You may observe these phases in Figure 3. Ppv1 and Ppv2, which are also represented as P V1 and P V2, are the power levels at MPP. It is reasonable to presume that the average power consumed by Co1 and Co2, Pco1 and Pco2, during a half-cycle is equivalent to the power obtained from P V1 and P V2, assuming that losses at the power processing stage are disregarded and that each subarray is operated at its maximum power point (MPP). As a result,

$$Pco1=Ppv1\&Pco2=Ppv2 \quad (1)$$

The typical half-cycle power delivered to the grid is denoted as Pg.

$$Pg=Ppv1+Ppv2 \quad (2)$$

5. CONTROL STRATEGY OF THE PROPOSED SCHEME

The control technique of the proposed approach is illustrated in the accompanying image. Fifthly, i) The current ig is sinusoidal and in phase with the voltage vg throughout the entire operational range. ii) Output voltage

sensing eliminates the need for vco1 and vco2. iii) Both subarrays operate simultaneously at their respective MPPs. The controller's development was influenced by the following objectives.

Two maximum power point (MPP) trackers and two proportional integral (PI) controllers are employed to determine Ppv1 and Ppv2, respectively, in order to estimate Vco1m and Vco2m. Equation (12) calculates Vco1m and Vco2m, while the phase-locked loop (PLL) determines Vm. Following the synchronization of a unity sinusoidal function (X) with voltage gain (vg), the same PLL produces a rectified version of the function (R). We can approximate vco1 and vco2 by multiplying R by Vco1m and Vco2m.

The calculations will not include the two voltage sensors required to differentiate between vco1 and vco2. The mode of operation of CONV1 can be ascertained by comparing Vpv1 and Vco1, whereas the mode of operation of CONV2 can be ascertained by comparing Vpv2 and Vco2. The emulated effective resistances, Rpco1 and Rpco2, of the two component converters can be determined by dividing the squared estimated RMS values of vco1 and vco2 by Ppv1 and Ppv2, respectively. The reference currents iL1ref for L1 and iL2ref for L2 are generated in buck mode by executing (28) in subsequent phases.

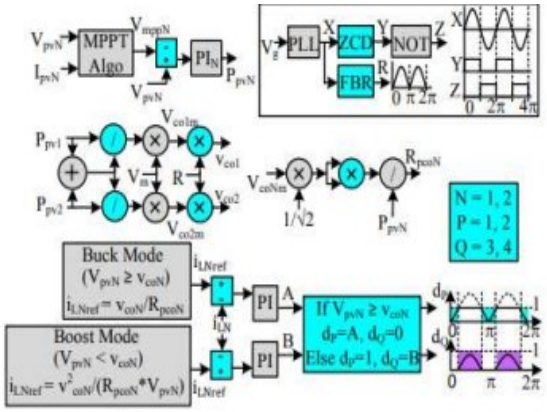

Fig. Control configuration of the proposed inverter

6.SIMULATION RESULTS

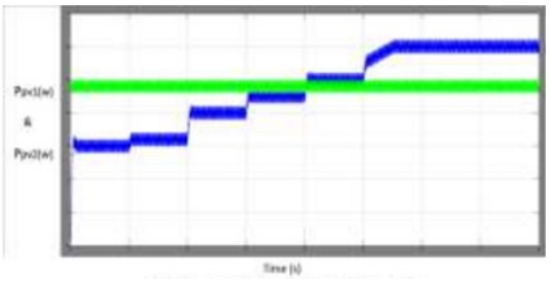

Fig : Simulated Waveform Variations in Ppv1 and Ppv2

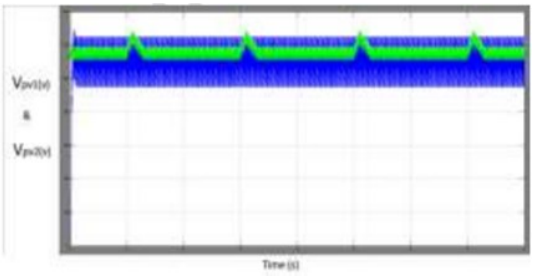

Fig : Simulated Waveform Variation in Vpv1 and Vpv2 during wide range of operation

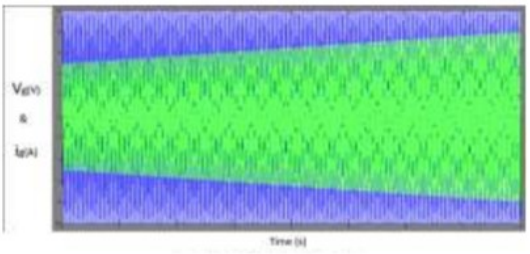

Fig : Simulated Waveforms of Vo and Io

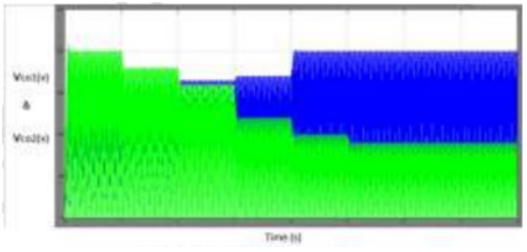

Fig: Simulated Waveforms of Vdc1 and Vdc2

7.CONCLUSION

This research proposes a transformerless buck-boost solar converter that can supply two subarrays at their respective optimum power points when connected to a single-phase grid. The inverter's numerous advantages, such as its high operational efficiency (ηeuro = 97.02%), its resilience to severe environmental conditions, its capacity to maintain the component converters' maximum power point (MPPT) through a user-friendly MPPT algorithm, and its ability to maintain the leakage current from the photovoltaic arrays below the VDE 0126-1-1 standards, enabled the decoupled component converter control. The compact signal model of the proposed inverter was established as a result of the mathematical research. The output filter's component selection was deliberated. The plan's feasibility was confirmed through a comprehensive modeling analysis and rigorous testing of a 1.5 kW prototype inverter that was specifically designed for this purpose.

REFERENCES

1. T. Shimizu, O. Hashimoto, and G. Kimura, “A novel high-performance utility-interactive photovoltaic inverter system,” IEEE Trans. Power Electron., vol. 18, no. 2, pp. 704-711, Mar. 2003.
2. S. V. Araujo, P. Zacharias, and R. Mallwitz, “Highly efficient single phase transformer less inverters for grid-connected photovoltaic systems,” IEEE Trans. Ind. Electron., vol. 57, no. 9, pp. 3118-3128, Sep. 2010.
3. B. Ji, J. Wang, and J. Zhao, “High-efficiency single-phase transformer less PV H6 inverter with hybrid modulation method,” IEEE Trans. Ind. Electron., vol. 60, no. 5, pp. 2104-2115, May 2013.
4. R. Gonzalez, E. Gubia, J. Lopez, and L. Marroyo, “Transformer less single phase multilevel-based photovoltaic inverter,” IEEE Trans. Ind. Electron., vol. 55, no. 7, pp. 2694-2702, Jul. 2008.
5. H. Xiao and S. Xie, “Transformer less splitinductor neutral point clamped three-level PV gridconnected inverter,” IEEE Trans. Power Electron., vol. 27, no. 4, pp. 1799-1808, Apr. 2012.
6. Bidram, A. Davoudi, and R. S. Balog, “Control and circuit techniques to mitigate partial shading effects in photo voltaic arrays,” IEEE J. Photovolt., vol. 2, no. 4, pp. 532-546, Oct. 2012.